Development of the mechanical properties of an Ultra-High Performance Fiber Reinforced Concrete (UHPFRC)

Katrin Habel [a,*], Marco Viviani [b], Emmanuel Denarié [c], Eugen Brühwiler [c,1]

[a] *University of Toronto, Department of Civil Engineering, 35 Street George Street, Toronto, ON, Canada, M5S 1A4*
[b] *GCC Technology and Processes, Avenue des sciences 1/A CH-1400 Yverdon les Bains, Switzerland*
[c] *Maintenance and Safety of Structures, Ecole Polytechnique Fédérale de Lausanne (EPFL), CH-1015 Lausanne, Switzerland*

Abstract

Knowledge of the mechanical properties, i.e. strength, stiffness and deformation capacity, of cementitious materials at any arbitrary time is fundamental for operations such as removal of formwork, prestressing or cracking control. This paper presents a study of the evolution of indexes related to hydration and their correlation to the development of the mechanical properties for an Ultra-High Performance Fiber Reinforced Concrete (UHPFRC). The hydration kinetics was determined using semi-adiabatic heat of hydration tests, and the mechanical properties were investigated experimentally at several ages between 3 and 365 days and then described with models originally developed for conventional concretes. Models and experiments were in good agreement. Furthermore, it was observed that for the UHPFRC, the rate of development of mechanical properties was highest for the secant modulus, followed by the compressive and then the tensile strength.
© 2006 Elsevier Ltd. All rights reserved.

1. Introduction

The development of the mechanical properties is fundamental for the design and construction of structures made of cementitious materials. Also, early age cracking is highly dependent on the development of stiffness and tensile properties. The strength development influences the construction process, for example the time of formwork removal and prestressing. At higher ages, the development of mechanical properties has a beneficial effect on the carrying capacity and stiffness of structures.

Ultra-High Performance Fiber Reinforced Concretes (UHPFRC) are cementitious composites with outstanding material properties [1–6]: they have very high strengths (compressive strength > 150 MPa, tensile strength > 8 MPa)

and exhibit strain-hardening behavior under uniaxial tension. The extremely low permeability of the dense matrix allows the use of UHPFRC, for example, as a waterproofing layer in bridge decks [7]. For practical and economical reasons, only UHPFRC without heat and pressure curing can be used in field applications.

This paper describes the experimental determination and the modeling of the development of the mechanical properties of a specific type of UHPFRC (CEMTEC$_{multiscale}$® [3,4]). A primary objective was to investigate whether existing models, developed for conventional concretes, could be adapted for UHPFRC with their low water/binder-ratios and their high silica fume content. Differences in the development of various mechanical properties of the UHPFRC are discussed. The behavior of the UHPFRC was also compared to conventional concretes.

For this, compressive and tensile properties at different ages as well as the heat of hydration were determined in an experimental program. Thermodynamic constants were determined as a function of the heat of hydration, and the development of the mechanical properties was modeled on the basis of the degree of reaction and then discussed.

* Corresponding author.
E-mail addresses: habel@ecf.utoronto.ca (K. Habel),
emmanuel.denarie@epfl.ch (E. Denarié), eugen.bruehwiler@epfl.ch
(E. Brühwiler).
[1] Tel.: +41 21 693 28 82; fax: +41 21 693 58 85.

2. Literature review

2.1. UHPFRC properties

The mix design of UHPFRC differs significantly from that of normal and high-strength concretes: UHPFRC mix compositions are characterized by high cement, superplasticizer and silica fume contents. Furthermore the water-binder ratio is lower than $w/b = 0.20$ [1–3,8]. The size of the coarsest aggregate used in UHPFRC generally lies between 0.5 and 4 mm. Strain-hardening behavior is achieved by incorporating a high percentage of steel fibers (more than 2 vol.%).

The high percentage of silica fume in the UHPFRC ($\approx 25\%$ of cement weight) changes the hydration kinetics and the mechanical properties. The hydration reaction of UHPFRC of the Reactive Powder Concrete (RPC) type was studied at very early age by Morin et al. [9,10]. They observed a long dormant period of about 30 h after water addition which was attributed to the high amount of superplasticizer. Then, the hydration started and was characterized by a strong heat release, which lasted for about 12 h. The degree of hydration was 18% at 70 h. Similar behavior was observed for cement pastes and high strength concretes for which the reaction started after a dormant period of 24 h followed by an intense hydration phase of 12 h [11,12].

Silica fume acts as a microfiller in UHPFRC. It also reacts with calcium hydroxide, thus increasing the final strength. Another important effect of the silica fume is the improvement of the interfacial transition zones between binder and aggregates and between binder and steel fibers [13–18].

The compressive strength of non-heat-treated water-cured and heat-treated not water-cured Ultra-High-Performance Concretes (UHPC) was investigated at several ages, indicating significant strength increase during the first months [19]. The strength gains for non-heat-treated and heat-treated Ultra-High-Performance Concretes amounted to additional 40% and 10% respectively for the period between 7 and 56 days. In another study, the strength increase of heat-cured UHPFRC was 5% between 28 and 200 days and another 5% between 200 and 400 days while the strength increase of air cured UHPFRC was 5% between 35 and 91 days and another 10% between 91 and 400 days [4].

2.2. Modeling the development of mechanical properties

The development of the mechanical properties has been widely studied for conventional concretes. Strength development is generally described as a function of indexes such as maturity, equivalent time and by the degrees of hydration and reaction. All these indexes have the scope of computing the combined effect of time, temperature and sometimes also humidity in concrete and thus to describe the progress of hydration at any time.

It has been shown that the mechanical properties of concrete are a function of the degree of hydration at a given time t, independently of the reaction rate. Thus, if a concrete mix with the same composition is cast several times and cured under sealed conditions at different curing temperatures, the degree of

hydration develops faster for the specimen cured at a higher temperature. Furthermore, for the same degree of hydration, all specimens have the same mechanical properties [20].

Degree of hydration indexes (DRI), such as maturity and equivalent time (see Eq. (1)) are commonly used to account for the advancement of the hydration process and to determine the development of mechanical properties versus DRI in the laboratory (i.e. determining thermodynamic constants such as the activation energy E in Eq. (1) and strength at any age). For a concrete member, the DRI can be computed at any time (see e.g. Eq. (1)) by measuring the temperature evolution during hydration in the member. Then, the mechanical properties of the member can be determined from DRI-strength curves established in the laboratory.

The strength development as a function of a DRI is generally modeled by hyperbolic [21] or exponential equations [22]. Maturity considers the temperature history of the cementitious material by integrating the temperature over time. The temperature history of the specimen can also be taken into account by calculating an equivalent time at a reference temperature that usually corresponds to 20 °C [23]. It is generally described by an Arrhenius-type equation (Eq. (1)) proposed by Hansen and Pedersen [24]:

$$t_{eq} = \sum e^{-\frac{E}{R}\left(\frac{1}{T(t)} - \frac{1}{T_{ref}}\right)} \cdot \Delta t \qquad (1)$$

where

t_{eq}	equivalent time
E	apparent activation energy (J/mol)
R	universal gas constant (8.314 J/(mol. K))
$T(t)$	temperature (K)
T_{ref}	reference temperature (usually 293 K)
Δt	time increment

The Arrhenius-type equation appears to better account for the effect of temperature on binder hydration than the linear Nurse–Saul maturity function [25,26] as shown in comparative studies (e.g. [27,28]).

Also, degree of hydration (or degree of reaction)-based models are commonly used to describe the development of mechanical properties [27,29–32]. Linear and power-type curves have been proposed that can be expressed by the following general equation (Eq. (2)) for any mechanical property "p":

$$\frac{p(r)}{p(r=1)} = \left(\frac{r-r_0}{1-r_0}\right)^a \qquad (2)$$

where

p	considered mechanical property (−)
r	degree of reaction (−)
r_0	degree of reaction at the beginning of the strength development (−)
a	parameter (−)

The degree of hydration describes the percentage of the initial binder that has hydrated at a given time t. The degree of reaction r indicates the evolution of the hydration reaction and is expressed as a percentage of the final degree of hydration (Eq. (3)). It is equal to $r=1$, when the final degree of hydration is reached.

$$r(t) = \frac{\alpha(t)}{\alpha(t \rightarrow \infty)} = \frac{\alpha(t)}{\alpha_{\text{final}}} \qquad (3)$$

where

α degree of hydration
α_{final} final degree of hydration
t time

Full cement hydration (i.e. $\alpha=1$) can be achieved in mixes with a water/cement-ratio higher than 0.42 according to Powers and Brownyard [33]. In this case, the degree of reaction is equal to the degree of hydration. For lower water/cement-ratios, part of the cement remains unhydrated as inert filler and the degree of reaction is higher than the degree of hydration. This is the case for high-strength concretes and UHPFRC.

The degree of hydration can be measured by direct methods such as X-ray diffraction analysis or SEM image analysis or indirectly by methods such as the amount of chemically bound water (overview e.g. in [34]).

The final degree of hydration can be predicted on the basis of the concrete mix composition. The extended Powers' model by Jensen [35] and the model proposed by Waller [36] consider both cement and silica fume reaction and are described in Appendix A.

In the extended Powers' model, the silica fume is assumed to react proportionally to the cement. The theoretical final degree of hydration is reached in cementitious materials with low water/binder-ratios when all the capillary water is consumed.

The degree of hydration in the Waller model is deduced from considerations of the heat release during hydration and the water/cement-ratio. Furthermore, the model takes into account the contributions of silica fume or fly ash. The Waller model allows the independent determination of the degrees of hydration for the cement and the pozzolan used.

In good approximation, the degree of reaction is commonly related to the heat of hydration by Eq. (4).

$$r(t) = \frac{Q(t)}{Q(t \rightarrow \infty)} = \frac{Q(t)}{Q_{\text{tot}}} \qquad (4)$$

where

Q cumulated heat of hydration
Q_{tot} total heat of hydration

The heat of hydration may be modeled with global models or by considering separately the heat release of every main clinker phase and the silica fume. The global models generally use exponential [24] or hyperbolic formulations, as used in this study (Eq. (5)) [21].

$$Q = Q_{\text{tot}} \cdot \frac{k(t_{\text{eq}}-d)}{1 + k(t_{\text{eq}}-d)} \qquad (5)$$

where

k rate constant
d dormant period

By using the relations in Eqs. (4) and (5), the degree of reaction can be calculated with the following equation (Eq. (6)):

$$r = \frac{k(t_{\text{eq}}-d)}{1 + k(t_{\text{eq}}-d)} \qquad (6)$$

Models based on the binder composition consider the hydration kinetics in more detail and need more precise knowledge about the chemical composition of the binder (e.g. [36,37]).

3. Experimental program

The self-compacting UHPFRC investigated in this study belongs to the family CEMTEC$_{\text{multiscale}}$® [3,4]. It had one type of short, straight steel fibers. Its detailed composition is given in Table 1. The cement used was a CEM I 52.5 with a relatively low C_3A-content and a low Blaine fineness (Table 2). White silica fume from the zirconium industry with a very low specific BET-surface was added, amounting to 26% of the cement weight. The superplasticizer was a polycarboxylate with modified phosphonates.

An extensive test program was conducted in order to describe the mechanical and time-dependent properties of the studied UHPFRC. The *heat of hydration* was determined with semi-adiabatic tests on cylindrical specimens (∅ 16 cm, height 32 cm). In parallel, the evolution of the *relative humidity* in the material was recorded in a sealed specimen under isothermal conditions at $T=20$ °C. The relative humidity was constant at 100% until 32 h after the addition of water and then decreased monotonically [38]. Also, linear-free and restrained autogenous shrinkage tests were performed on early age UHPFRC from casting on. The relative humidity and autogenous shrinkage tests were only used in this study to determine the beginning of hardening of the UHPFRC. A more detailed description of the test procedures and results can be found in [38].

Table 1
Composition of the UHPFRC

Constituent	Type	Weight [kg/m³]
Cement	CEM I 52.5 N	1050
Quartz sand	Diameter <500 μm	730
Silica Fume	Spec. surf.: 12 m²/g	275
Steel fibers	Straight (10 mm, 0.2 mm)	470
Superplasticizer	Chryso Optima 175	35
Total water		190

Mineralogical composition	
C_2S	73.4%
C_3S	10.0%
C_3A	4.0%
C_4AF	5.8%
Specific surface (Blaine fineness)	3400 cm^2/g

Compressive strength and secant modulus at 30% of the compressive strength were determined on cylindrical specimens (∅ 11 cm, length 22 cm) after standard testing procedures. Tests were performed at 4, 8, 15, 28, 90 and 365 days on three specimens at each time. The compressive strength was f_{Uc} = 168 MPa and its secant modulus E_{Uc} = 48 GPa at 28 days. All specimens were demoulded after three days and then water-cured at 20 °C until testing.

The *tensile properties* were determined with a uniaxial tensile test on notched plates having a cross-section of 20 * 5 cm^2 and a reduced cross-section of 16 * 5 cm^2 at the notches [6]. Tests were conducted at 4, 8, 15, 28, 90 and 365 days. The tensile behavior of the tested UHPFRC was characterized by significant strain-hardening (Fig. 1). The first cracking strength of the UHPFRC was $f_{Ut,1st}$ = 9.1 MPa, the tensile strength $f_{Ut,max}$ = 11.0 MPa and the fracture energy G_{FU} = 20.2 kJ/m^2 at 28 days. The first cracking strength is hereby defined as the stress when first distributed macrocracks of small widths form, i.e. at the beginning of strain hardening. The tensile strength is the maximum strength at the end of the strain-hardening domain. In addition, the strain at the tensile strength $\varepsilon_{Ut,max}$ as well as the secant modulus at the beginning of the test E_{Ut} were determined for each specimen. The specific fracture energy G_{FU} was assumed to be equal to the work of fracture (area under the force-displacement-curves) during the tensile test, divided by the ligament area. The test specimens were demoulded after three days and then water-cured at 20 °C until testing.

4. Results and discussion

4.1. Degree of hydration and degree of reaction

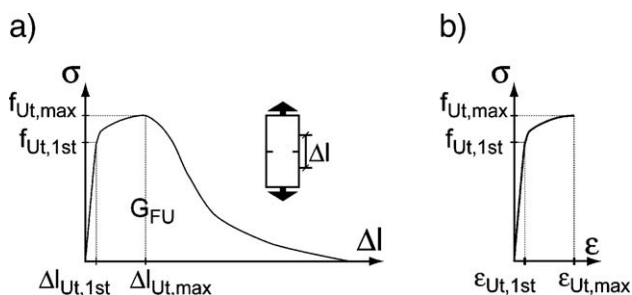The development of the hydration reaction of the UHPFRC was determined by using experimental data and existing

models: the reaction kinetics was evaluated with a technique that used semi-adiabatic heat of hydration tests to describe the hydration process. The setting point was established based on the relative humidity and autogenous shrinkage tests. The final degree of hydration, i.e. the final amount of hydrated binder, was calculated with the extended Powers' model of Jensen [35] and the Waller model [36] (Appendix A). Within the scope of this article, a distinction is made between the degree of hydration and the degree of reaction, as described in Section 2.

The theoretical total degree of hydration of the investigated UHPFRC, calculated with the extended Powers' model for a closed system, which considers the reaction of cement and silica fume together, amounted to α = 0.31 (see Appendix A). The assumption of a closed system for the UHPFRC is realistic, since tests have shown that the dense matrix of UHPFRC prevents the ingress of water [38]. The cement and silica fume final degrees of hydration were evaluated separately with the Waller model, giving final values of α_c = 0.31 and α_{SF} = 0.30 respectively. The assumption of the extended Powers' model that cement and silica fume hydrate proportionally is found to be consistent with the results given by the Waller model with respect to the final degree of hydration. Considering the results of the two models, the final degree of hydration of the binder (silica fume and cement) for the studied UHPFRC was assessed to be α = 0.31.

The low final degree of hydration is explained by the low water-binder-ratio of the UHPFRC, causing self-desiccation. In addition, the amount of water is not sufficient to lead to full hydration of the binder.

The evolution of hydration is described by the degree of reaction that was deduced from the results of the semi-adiabatic heat of hydration tests. For this, it was assumed that the released heat is proportional to the hydration reaction as shown in Eq. (4), and the hyperbolic model of Eq. (6) was fitted to the experimental results. This model is well established for conventional and for slag cement concretes and has successfully been used in field applications [39].

Fig. 1. Tensile behavior of UHPFRC: a) schematic test results, b) definition of the hardening behavior.
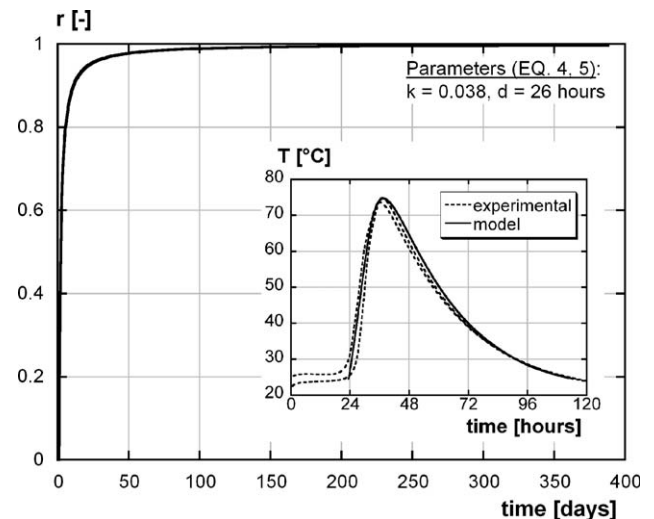

Fig. 2. Development of the degree of reaction with time, detail: experimental results of the semi-adiabatic heat of hydration tests and modeling.
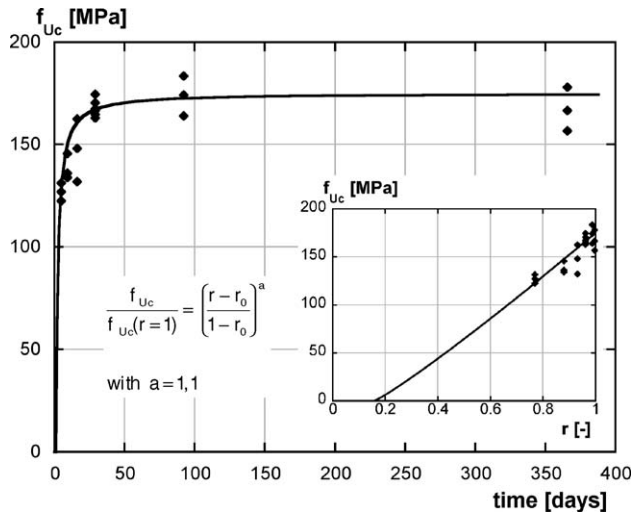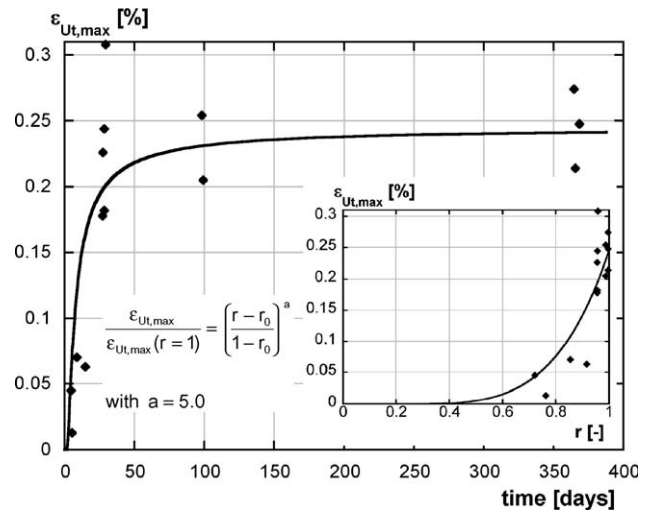
Fig. 3. Compressive strength ($R^2 = 0.93$).

Fig. 5. Strain at the tensile strength ($R^2 = 0.79$).

A dormant period of $d = 26$ h was determined by fitting the hyperbolic model to the semi-adiabatic heat of hydration test results (Fig. 2), since it was assumed that the reaction started with a strong heat release after 26 h of virtually constant temperature. The investigated UHPFRC exhibited a strong increase in the degree of hydration reaction r at early age: the degree of reaction amounted to $r = 0.63$ at 3 days and $r = 0.84$ after 7 days. Degrees of reaction of $r = 0.96$ after 28 days and $r = 0.99$ after 90 days indicate that the hydration reaction was virtually finished at 90 days.

The setting point is observed macroscopically when the material properties start to develop. In this study, it was assumed that setting occurred when the material showed an apparent stiffness higher than 1 GPa and when self-desiccation started. This was observed during the relative humidity and the autogenous shrinkage tests between 31 and 32 h for the investigated UHPFRC [38]. Thus, the degree of reaction at the setting point was determined to be $r_0 = r$ (31.5 h) $= 0.16$.

4.2. Development of mechanical properties

4.2.1. Overview

The time development of the mechanical properties of the UHPFRC was converted into DRI-histories using the equivalent time as DRI according to Eq. (6). Then the power-type model in Eq. (2) was fitted to the data, and the results were compared.

Figs. 3–7 show the test results and the fitted parameter a of the power-type model of Eq. (2). The higher the parameter a in the fit, the slower is the evolution of the specific mechanical property as a function of the degree of reaction. The summary of the results as well as the regression coefficient R^2 are shown in Table 3.

Five groups of mechanical properties were distinguished:

– *Compressive strength* f_{Uc}. It was modeled with $a = 1.1$.
– *Tensile strength*, consisting of the first cracking strength $f_{Ut,1st}$ and the tensile strength $f_{Ut,max}$. Here, the power-type function of Eq. (2) with $a = 2.5$ was the best fit.
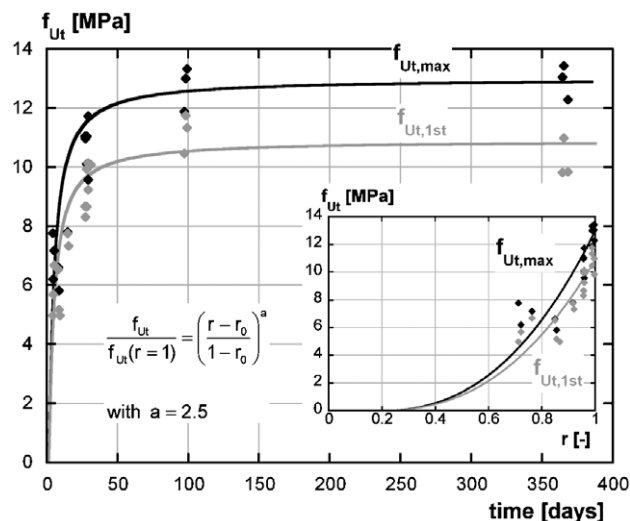

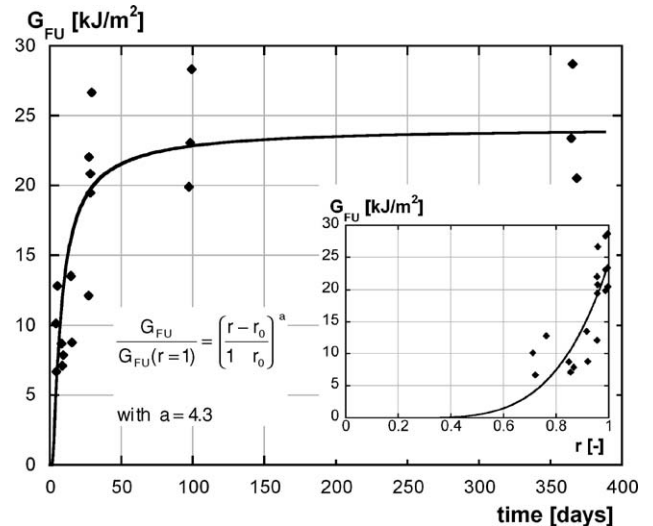Fig. 4. Tensile strength ($f_{Ut,max}$: $R^2 = 0.76$, $f_{Ut,1st}$: $R^2 = 0.85$).
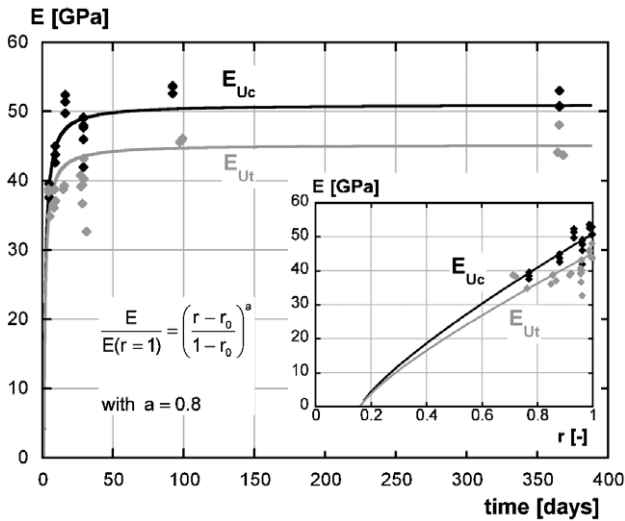

Fig. 6. Fracture energy ($R^2 = 0.72$).

Fig. 7. Secant modulus (E_{Uc}: $R^2 = 0.94$, E_{Ut}: $R^2 = 0.82$).

– *Hardening*, consisting of the strain at the tensile strength $\varepsilon_{Ut,max}$. Here, the power-type function of Eq. (2) was the best fit with $a = 5.0$.
– *Fracture energy* G_{FU}, with the power-type function of Eq. (2), being fitted to $a = 4.3$.
– *Stiffness*, consisting of the secant modulus under compression E_{Uc} and under tension E_{Ut}. This group is called stiffness, since both properties are related with the deformation capacity of the UHPFRC in its quasi-linear elastic state. The power-type function of Eq. (2) was best fitted to $a = 0.8$.

4.2.2. Correlation coefficients

The correlation coefficients from the regression analysis generally indicate good agreement between the test results and the proposed model with values between $R^2 = 0.72$ and 0.94. The coefficients for the compression properties (f_{Uc}, E_{Uc}) ($R^2 = 0.93$ and 0.94) were higher than the ones for the tensile properties ($f_{Ut,max}$, $f_{Ut,1st}$, $\varepsilon_{Ut,max}$, E_{Ut}, G_{FU}) ($R^2 = 0.72$ to 0.85).

The lower correlation coefficients for the tensile properties may be due to the large scatter of the tensile tests at a given age, rather than due to inadequate modeling of the time-dependent development of the mechanical properties. The scatter in tensile properties may be explained by some variation in the fiber distribution, as already shown in [6].

The highest correlation coefficients of the tensile properties ($R^2 = 0.85$) were found for the first cracking strength $f_{Ut,1st}$ as well as for the secant modulus E_{Ut} ($R^2 = 0.85$). Both properties were closely related to the strength of the matrix. Lower coefficients were determined for the tensile properties after the formation of distributed macrocracks in the matrix ($R^2 = 0.72$ to 0.79), where the steel fibers are strongly involved in the fracture mechanism. This indicates high sensitivity of the tensile properties of UHPFRC to inhomogeneities in the fiber distribution.

4.2.3. Comparison of the evolution of the different mechanical properties

The results show that the secant moduli E_{Uc} and E_{Ut} developed at the highest rate with a parameter $a = 0.8$, followed

by the compressive strength ($a = 1.1$) and the tensile properties ($a \geq 2.5$).

The differences in the development of the mechanical properties may be explained by the mix composition. The UHPFRC had a very low final degree of hydration with $\alpha \approx 0.31$, indicating that the major part of the binder did not hydrate, but acted as filler. Thus, a high compacity of the matrix was obtained, resulting in high strengths and very low permeability [1,2,40]. The reacted part of the binder built the skeleton and provided bond between the steel fibers and the matrix. The silica fume reaction is generally very fast in the beginning and then slows down considerably [41]. Thus, the observed rapid development of secant moduli and compressive strength suggests that the initial formation of hydration products is determinant for these two properties and that the later formed bonds are less important. The importance of silica fume on the strength development from early ages on was demonstrated previously [16,42].

The relatively slow development of the tensile properties may be attributed to the binder reaction and to the interaction between steel fibers and matrix. The tensile properties are likely to be sensitive to the different chemical reactions and rearrangements during the full period of hydration as observed by Sarkar and Aïtcin [11]. The reactions during later stages of hydration seem to contribute even more significantly to the strength increase in the material.

The bond of the steel fibers is improved by the silica fume leading to a significant reduction of the interface transition zone (ITZ) [16], an enhancement of the interfacial bond and to a reduction of weaknesses at the interface [13,18]. In binders with high silica fume contents, more particles adhere to the steel fibers on the microstructural level and thus, the pull-out energy is significantly increased [43]. It is likely that these adhered particles and the resulting mechanical interlock only become important for higher degrees of hydration, when the new hydration products fill out small gaps in the matrix and densify the matrix further on the microstructural level [15,17]. This may explain the relatively slow development of the hardening strain $\varepsilon_{Ut,max}$ and the fracture energy — the two tensile properties that were influenced most by the steel fibers. However, further studies are necessary to confirm these findings.

4.2.4. Consequences of the evolution of the mechanical properties

The fast development of the degree of reaction also led to a fast development of the mechanical properties. Thus, at 7 days, the concrete compressive strength f_{cc} amounted to 140 MPa,

Table 3
Fitting of the development of the mechanical properties ($r_0 = 0.16$)

Group	Property	a [-]	Property at $r = 1$	R^2 [-]
Compressive strength	f_{Uc}	1.1	175.0 MPa	0.93
Tensile strength	$f_{Ut,max}$	2.5	13.0 MPa	0.76
	$f_{Ut,1st}$	2.5	10.9 MPa	0.85
Hardening	$\varepsilon_{Ut,max}$	5.0	0.027%	0.79
Fracture energy	G_{FU}	4.3	24.2 kJ/m^2	0.72
Stiffness	E_{Uc}	0.8	51.0 GPa	0.94
	E_{Ut}	0.8	45.2 GPa	0.82

which was 81% of the final strength (for a degree of reaction $r=1$); the tensile strength $f_{Ut,max}$ was 5.8 MPa, corresponding to 60% of the final strength and the secant modulus E_{Uc} was 42.7 GPa, corresponding to 84% of the final modulus.

The high early strengths are advantageous to accelerate the construction process. However, the slow development of the UHPFRC tensile properties, when compared to the development of the secant modulus, means a certain early age cracking risk in the case of deformation restraint. On the other hand, the investigated UHPFRC showed a tensile strength three times higher than conventional concretes; and additionally, UHPFRC exhibited pronounced strain-hardening behavior under uniaxial tension. Internally caused early age deformations are of the same order of magnitude as for conventional concretes [38], and numerical simulations showed that no large cracks (>50 μm) form in the UHPFRC even under totally restrained conditions, which was confirmed by long-term tests on highly restrained UHPFRC [44]. From this follows that the risk of early age cracking of UHPFRC in composite systems is rather low.

The rapid development of the mechanical properties and the virtual completion of hydration at 90 days for neither heat- nor pressure-treated UHPFRC may also influence the construction process. For example, a newly built composite "UHPFRC-concrete" bridge can already be subjected to live loads at 7 days, if some load limitation is respected. Moreover, the virtual stop of hydration of the UHPFRC after 90 days leads to a structure with final, constant material properties for higher ages.

4.3. Degree of reaction as determinant state variable

The development of the mechanical properties of UHPFRC was successfully described by using models commonly applicable for conventional concretes. The degree of reaction is also the determinant state variable for this evolution for cementitious composites with very low water/binder-ratios and high percentages of silica fume, as this was the case for the given UHPFRC. Consequently, the results show that silica fume and cement reaction can be described with a global degree of reaction. This was confirmed by the fact that silica fume and cement reached similar final degrees of hydration as shown by the Waller model.

4.4. Comparison to conventional concretes

UHPFRC has significantly improved properties with regard to mechanical performance and durability when compared to conventional concrete. However, both are cementitious materials based on principally similar chemical reactions during hydration. In this section, differences and similarities concerning the reaction kinetics between UHPFRC and conventional concretes are discussed.

The differences in the mix design between UHPFRC and conventional concretes also result in some important differences in the mechanical properties and in the reaction kinetics: Most importantly, the development of the mechanical properties of the studied UHPFRC practically reached its final value at an age of 90 days, while the development of conventional concretes

usually takes several decades — the strength of conventional concrete at 30 years or more was reported to be up to 2 to 3 times higher than at 28 days [41]. An experimental study by the authors showed that the compressive strength and the secant modulus of water-cured cylinders made of conventional concrete increased by 16% and 6% respectively between 90 and 365 days [6].

The virtual end of the development of the mechanical properties corresponded to the virtual completion of the hydration reaction at 90 days ($r=0.99$). The low water-binder-ratio of the UHPFRC allows only partial hydration of the binder and leads to self-desiccation [38]. The hydration reaction virtually stopped at 90 days, shown by the degree of reaction for the UHPFRC at this age that was determined to be $r(90\ days)=0.99$. In contrast, full hydration is possible in conventional concretes with water/cement-ratios higher than $w/c=0.42$, and the hydration reaction continues for several decades for these concretes.

The faster rate of the development of the degree of reaction of the UHPFRC also leads to higher early age strengths and stiffness when compared to conventional concrete. This advantage of UHPFRC may be used to accelerate the construction process and prestressing. Moreover, the UHPFRC may be seen as inert after only three months with all its mechanical properties becoming virtually constant at that age.

The degree of reaction was found to be the determinant variable for the description of the development of the mechanical properties of UHPFRC and for conventional concrete. Also, the initial degree of reaction, i.e. the degree of reaction when the mechanical properties started to develop, was similar for conventional concretes and UHPFRC. It amounted to $r_0=0.16$ for the UHPFRC of this study and to values between 0.10 and 0.30 for conventional concretes [30–32,45]. This indicates a similar threshold of strength development at very early age. However, the dormant period of 26 h of the investigated type of UHPFRC was significantly longer than that of conventional concrete. This was attributed to the setting retarding effect due to the high amount of superplasticizer in the UHPFRC [6,9].

The compressive strength-DRI development of the UHPFRC ($a=1.1$) and conventional concretes ($a=0.84–1.5$ [27,30,31,46]) are comparable. However, the development of the stiffness, expressed by the secant modulus, was slower for the studied UHPFRC ($a=0.8$) than for conventional concretes ($a=0.26–0.62$ [30,31,46]).

The main difference between UHPFRC and conventional concrete is observed in the development of the tensile properties: for conventional concrete, the tensile strength develops at a higher rate than the compressive strength and at a lower rate than the secant modulus ($a=0.46–1.0$ for conventional concrete [30,31,46]). In contrast, the increase in tensile properties ($a=2.5–5.0$) was slower than that of the secant modulus and the compressive strength for the studied UHPFRC. An even bigger difference was observed for the fracture energy with $a=1.0$ for conventional concrete [47] and $a=5.0$ for the investigated UHPFRC. This may be attributed to the beneficial effect of the silica fume reaction on strength and interface transition zone of the UHPFRC as already discussed previously.

5. Conclusions

The development of the mechanical properties with time was investigated for a UHPFRC belonging to the family CEMTEC$_{multiscale}$® [3], without heat treatment on the basis of compressive and tensile tests at 4, 8,15, 28, 90 and 365 days. The following conclusions can be drawn:

1. The development of the mechanical properties of the studied UHPFRC was successfully described by a degree of reaction-based formulation commonly used for conventional concrete. The degree of reaction was identified to be the determinant state variable also for the UHPFRC.
2. The hydration reaction started at 26 h after water addition and was retarded, which was due to the high amount of superplasticizer in the mix. The reaction rate was assumed to be proportional to the heat release during hydration and was described as a function of the degree of reaction with a power-type model commonly used for conventional concrete.
3. The mechanical properties started to develop at a degree of reaction of $r_0 = 0.16$ at approximately 32 h after the addition of water to the mix. The degree of reaction amounted to $r = 0.99$ after 90 days, indicating a virtual stop of the hydration reaction at this age. Also, the development of the mechanical properties virtually stopped after 90 days. This means that the UHPFRC can be assumed inert beyond this age.
4. The final degree of hydration of the UHPFRC was calculated to be $\alpha \approx 0.31$.
5. The development of the tensile properties of the UHPFRC was slower when compared to the compressive properties and the secant moduli.

Appendix A. Description of the extended Powers and the Waller model

A.1. Extended Powers model by Jensen [35]

The extended Powers model (for a closed system) by Jensen assumes that the reaction of silica fume is proportional to the cement reaction. It is based on the following equations:

$$\text{Chemical shrinkage} : V_{cs} = k(0.2 + 0.7(\text{SF}/c))(1-p)\alpha$$
$$\text{Capillary water} : V_{cw} = p - k(1.4 + 1.6(\text{SF}/c))(1-p)\alpha$$
$$\text{Gel water} : V_{gw} = k(0.6 + 1.6(\text{SF}/c))(1-p)\alpha$$
$$\text{Gel solid} : V_{gs} = k(1.6 + 0.7(\text{SF}/c))(1-p)\alpha$$
$$\text{Cement} : V_c = k(1-p)(1-\alpha)$$
$$\text{Silica fume} : V_{SF} = k(1.4(\text{SF}/c))(1-p)(1-\alpha)$$

where

$$\sum_1 V_i = 1$$

$$p = \frac{w/c}{(w/c) + (\rho_w/\rho_c) + (\rho_w/\rho_{SF})(\text{SF}/c)}$$

$$k = \frac{1}{1 + 1.4(\text{SF}/c)}$$

The constants in Powers' volumetric model are derived from the following data:

Non-evaporable water: $w_n = 0.23$ g/g cement reacted and $w_n = 0$ g/g silica fume reacted,

Gel water: $w_{gw} = 0.19$ g/g cement reacted and $w_{gw} = 0.5$ g/g silica fume reacted,

Chemical shrinkage: $\Delta V = 6.4$ ml/100 g cement reacted and $\Delta V = 20$ ml/100 g silica fume reacted.

w, c and SF refer to masses of water, cement and silica fume respectively, with $\rho_c \approx 3150$ kg/m^3, $\rho_{SF} \approx 2200$ kg/m^3 and $\rho_w \approx 1000$ kg/m^3.

The final degree of hydration is attained, when the capillary water V_{cw} is equal to zero, i.e. $\alpha = \frac{p}{k \cdot (1.4 + 1.6 \cdot (\text{SF}/c))(1-p)}$.

For the UHPFRC presented in this paper, the final degree of hydration was $\alpha = 0.31$ with SF/$c = 0.26$ and $w/c = 0.18$.

A.2. Waller model [36]

The model developed by Waller for cementitious materials considers the reaction of silica fume and cement with the following equations:

$$\alpha_c(\infty) = 1 - \exp\left(-3.3 \cdot \left(\frac{w}{c} - \delta\right)\right)$$

where

$$\delta = 0.6 \cdot \min\left[\frac{\text{SF}}{c}; \frac{x}{1.3} \cdot \alpha_c(\infty)\right] \cdot \exp\left(1.6 \cdot \frac{w}{c}\right)$$

quantity of lime: $x = 0.13 \ \varphi_{C2S} + 0.42 \ \varphi_{C3S}$

$$\alpha_{fs}(\infty) = \min\left[1; \frac{x \cdot \alpha_c(\infty)}{1.3 \cdot \frac{\text{SF}}{c}} \cdot \alpha_c(\infty)\right]$$

w, c and SF refer to masses of water, cement and silica fume quantities respectively, with given in [kg/m^3]; φ_{C2S} and φ_{C3S} represent the relative content of C$_2$S and C$_3$S in the cement.

The degree of hydration is calculated by solving the implicit equations. The input values for the UHPFRC discussed in this paper were: SF/$c = 0.26$, $w/c = 0.18$, $\varphi_{C2S} = 0.1$ and $\varphi_{C3S} = 0.734$. The degree of hydration of the cement was $\alpha_c = 0.31$ and the degree of hydration of the silica fume $\alpha_{SF} = 0.30$.

References

[1] H.H. Bache, Introduction to compact reinforced composite, Nord. Concr. Res. 6 (1987) 19–33.

[2] P. Richard, M. Cheyrezy, Composition of reactive powder concretes, Cem. Concr. Res. 25 (7) (1995) 1501–1511.

[3] P. Rossi, A. Arca, E. Parant, P. Fakhri, Bending and compressive behaviors of a new cement composite, Cem. Concr. Res. 35 (1) (2005) 27–33.

[4] E. Parant, Mécanismes d'endommagement et comportements mécaniques d'un composite cimentaire fibré multi-échelles sous sollicitations sévères: fatigue, choc, corrosion (Damage mechanisms and mechanical behaviour of a cementitious composite with multi-scale fibre reinforcement under severe load conditions), Doctoral thesis, Laboratoire Central des Ponst et Chaussées, Paris, France, 2003 (in French).

[5] J.-P. Charron, E. Denarié, E. Brühwiler, Permeability of UHPFRC under high stresses, Proceedings of RILEM Symposium, Advances in Concrete Through Science and Engineering, Evanston, Il, March 2004, p. 12.

[6] K. Habel. Structural behaviour of elements combining Ultra-High Performance Fibre Reinforced Concretes (UHPFRC) and Reinforced Concrete, Doctoral thesis 3036, Swiss Federal Institute of Technology Lausanne, Switzerland, 2004 (http://biblion.epfl.ch/EPFL/theses/2004/3036/EPFL_TH3036.pdf).

[7] E. Denarié, Structural rehabilitations with Ultra-High Performance Fibre Reinforced Concretes (UHPFRC), in: M. Alexander, H.D. Beushausen, F. Dehn, P. Moyo (Eds.), Proc Int Conf on Concrete Repair, Rehabilitation and Retrofitting (ICCRRR05), Taylor and Francis, London, 2005.

[8] F. de Larrard, T. Sedran, Optimization of Ultra-High-Performance Concrete by the use of a packing model, Cem. Concr. Res. 24 (6) (1994) 997–1009.

[9] V. Morin, F. Cohen Tenoudji, A. Feylessoufi, P. Richard, Superplasticizer effects on setting and structuration mechanisms of Ultra High-Performance Concrete, Cem. Concr. Res. 31 (1) (2001) 63–71.

[10] V. Morin, F. Cohen-Tenoudji, A. Feylessoufi, P. Richard, Evolution of the capillary network in a reactive powder concrete during hydration process, Cem. Concr. Res. 32 (12) (2002) 1907–1914.

[11] S.L. Sarkar, P.C. Aïtcin, Dissolution rate of silica fume in very high strength concrete, Cem. Concr. Res. 17 (4) (1987) 591–601.

[12] D.M. Roy, Hydration of blended cements containing slag, fly ash, or silica fume, Proceedings of Meeting Institute of Concrete Technology, Coventry, UK, 1987, 29 pp.

[13] N. Banthia, A study of some factors affecting the fiber-matrix bond in steel fiber reinforced concrete, Can. J. Civ. Eng. 17 (4) (1990) 610–620.

[14] D.P. Bentz, P.E. Stutzman, E.J. Garboczi, Experimental and simulation studies of the interfacial zone in concrete, Cem. Concr. Res. 22 (5) (1992) 891–902.

[15] D.D.L. Chung, Review: improving cement-based materials by using silica fume, J. Mater. Sci. 37 (4) (2002) 673–682.

[16] M.D. Cohen, A. Goldman, W.-F. Chen, The role of silica fume in mortar: transition zone versus bulk paste modification, Cem. Concr. Res. 24 (1) (1994) 95–98.

[17] A. Goldman, A. Bentur, Properties of cementitious systems containing silica fume or nonreactive microfillers, Adv. Cem. Based Mater. 1 (5) (1994) 209–215.

[18] H. Yan, W. Sun, H. Chen, The effect of silica fume and steelfiber on the dynamic mechanical performance of high-strength concrete, Cem. Concr. Res. 29 (3) (1999) 423–426.

[19] E. Fehling, M. Schmidt, T. Teichmann, K. Bunje, B. Bornemann, Entwicklung, Dauerhaftigkeit und Berechnung Ultra-Hochfester Betone (UHPC) (Development, durability and calculation of Ultra-High Strength Concretes (UHPC)), Research Report, Schriftenreihe Baustoffe und Massivbau 1, Kassel, 2004 (in German).

[20] A. Schindler, Effect of temperature on the hydration of cementitious materials, ACI Mater. J. 101 (1) (2004) 72–81.

[21] T. Knudsen, The dispersion model for hydration of portland cement: I. General concepts, Cem. Concr. Res. 14 (5) (1984) 622–630.

[22] P.F. Hansen, E.J. Pedersen, Curing of Concrete Structures, CEB Information Bulletin, vol. 166, Lausanne, Switzerland, 1985.

[23] E. Rastrup, Heat of hydration in concrete, Mag. Concr. Res. 6 (17) (1954) 79–92.

[24] P.F. Hansen, E.J. Pedersen, Måleinstrument til kontrol af betons hærdning (Maturity computer for controlled curing and hardening of concrete), Nord. Betong 1 (1997) 177–182 (in Danish).

[25] R.W. Nurse, Steam curing of concrete, Mag. Concr. Res. 1 (2) (1949) 79–88.

[26] A.G.A. Saul, Principles underlying the steam curing of concrete at atmospheric pressure, Mag. Concr. Res. 2 (6) (1956) 127–140.

[27] J. Byfors, Mechanical properties, Proceedings, RILEM International Conference on Concrete at Early Ages, vol. I, Ecole Nationale des Ponts et Chausses, Paris, France, 1982, pp. 13–33.

[28] N.J. Carino, Maturity functions for concrete, Proceedings, RILEM International Conference on Concrete at Early Ages, vol. I, Ecole Nationale des Ponts et Chausses, Paris, France, 1982, pp. 123–128.

[29] A. Boumiz, C. Vernet, F. Cohen Tenoudji, Mechanical properties of cement pastes and mortars at early ages, Adv. Cem. Based Mater. 3 (3–4) (1996) 94–106.

[30] G. de Schutter, L. Taerwe, Degree of hydration-based description of mechanical properties of early age concrete, Mat. Struct. 29 (190) (1996) 335–344.

[31] F.S. Rostasy, M. Laube, P. Onken, Zur Kontrolle früher Temperaturrisse in Betonbauteilen (About the control of early temperature cracks in concrete structures), Bauingenieur 68 (1) (1993) 5–14.

[32] J.-M. Torrenti, La résistance du béton au très jeune âge (Concrete strength at very early age), Bull. Liaison Lab. Ponts Chaussées, Paris, France 179 (1992) 31–41 (in French).

[33] T.C. Powers, T.L. Brownyard, Studies of the physical properties of hardened Portland cement paste, Research Laboratories, PCA Bulletin, vol. 22. Portland Cement Association (PCA), Chicago, Illinois, March 1948.

[34] K. van Breugel, Hydration of cement-based systems, Brite, EuRam Project, ICAPS-Improved Production of Advanced Concrete Structures, Delft, The Netherlands, 2001, p. 17-6.

[35] P. Lura, O.M. Jensen, K. van Breugel, Autogenous shrinkage in high-performance cement paste. An evaluation of basic mechanisms, Cem. Concr. Res. 33 (2) (2003) 223–232.

[36] V. Waller. Relations entre composition des bétons, exothermie en cours de prise et résistance à la compression (Relation between concrete composition, exothermy during setting and compressive strength), Doctoral thesis, Laboratoire Central des Ponst et Chaussées Nantes, France, 2000 (in French).

[37] O. Bernard, F.J. Ulm, E. Lemarchand, A multiscale-hydration model for the early-age elastic properties of cement-based materials, Cem. Concr. Res. 33 (9) (2003) 1293–1309.

[38] K. Habel, J.-P. Charron, E. Denarié, E. Brühwiler, Autogenous deformations and viscoelasticity of UHPFRC in structures: Part I. Experimental results, Mag. Concr. Res. 58 (3) (April 2006) 135–145.

[39] G. de Schutter, Applicability of degree of hydration concept and maturity method for thermo-visco-elastic behaviour of early age concrete, Cem. Concr. Compos. 26 (5) (2004) 437–443.

[40] F. de Larrard, Y. Malier, Propriétés constructives des bétons à très hautes performances — De la micro à la macrostructure, Annales de L'I.T.B.T.P 479, France, 1989, pp. 79–109 (in French).

[41] A. Neville, Properties of concrete, Pearson, Prentice Hall, Harlow, 1995.

[42] J.P. Ollivier, A. Carles-Gibergues, B. Hanna, Activité pouzzolanique et action de remplissage d'une fumée de silice dans les matrices de béton de haute résistance (Pozzolan activity and filling action of silica fume dans high strength concrete matrices), Cem. Concr. Res. 18 (3) (1988) 438–448.

[43] Y.-W. Chan, S.-H. Chu, Effect of silica fume on steel fiber bond characteristics in reactive powder concrete, Cem. Concr. Res. 34 (7) (2004) 1167–1172.

[44] K. Habel, E. Denarié, E. Brühwiler. Time dependent behavior of elements combining Ultra-High Performance Fiber Reinforced Concretes (UHPFRC) and Reinforced Concrete. Mater Struct (in press).

[45] K. van Breugel, Numerical simulation of hydration and microstructural development in hardening cement-based materials, Heron 37 (3) (1992) (Delft, the Netherlands).

[46] M.S. Sule, Effect of reinforcement on early-age cracking in high strength concrete, Doctoral thesis, Delft University, the Netherlands, 2003.

[47] G. de Schutter, L. Taerwe, Fracture energy of concrete at early age, Mat. Struct. 30 (196) (1997) 67–71.